Chemosphere 219 (2019) 1032–1043

Contents lists available at ScienceDirect

Chemosphere

journal homepage: www.elsevier.com/locate/chemosphere

Review

Isotope fractionation due to aqueous phase diffusion – What do diffusion models and experiments tell? – A review

Philipp Wanner [a, *], Daniel Hunkeler [b]

[a] College of Engineering and Physical Sciences, University of Guelph, 50 Stone Road East, Guelph, Ontario, N1G 2W1, Canada
[b] Centre for Hydrogeology & Geothermics (CHYN), University of Neuchâtel, Rue Emil Argand 11, CH-2000, Neuchâtel, Switzerland

HIGHLIGHTS

- Review of how five diffusion models predict isotope fractionation.
- Compilation of experimental studies addressing diffusive isotope fractionation.
- Diffusion models are inconsistent in their prediction of isotope fractionation.
- Experimental data reveals a weak power law mass dependency of D for most solutes.
- Experimental data is consistent with Mode-Coupling Theory Analysis of diffusion.

GRAPHICAL ABSTRACT

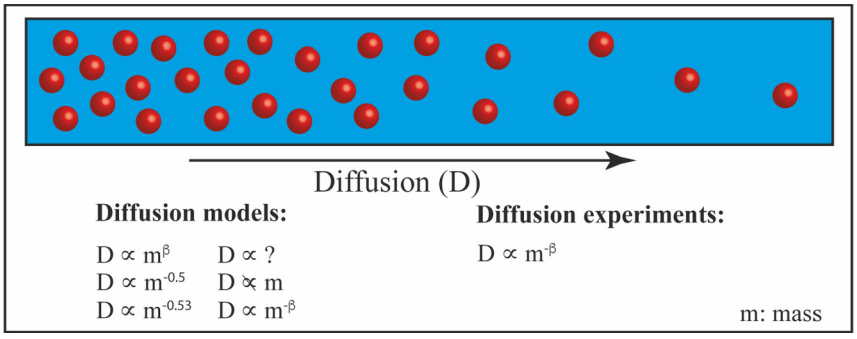

ARTICLE INFO

Article history:
Received 20 August 2018
Received in revised form
30 November 2018
Accepted 5 December 2018
Available online 7 December 2018

Handling Editor: Martine Leermakers

ABSTRACT

For the interpretation of stable isotope ratio trends in saturated geochemical systems, the magnitude of aqueous phase diffusion-induced isotope fractionation needs to be known. This study reviews how five diffusion models (Fick, Maxwell-Stefan, Einstein, Langevin, Mode-Coupling Theory Analysis (MCTA) of diffusion) predict isotope fractionation due to aqueous phase diffusion and compares them with experimental results. The reviewed diffusion models were not consistent regarding the prediction of the mass (m) dependency of the aqueous phase diffusion coefficient (D). The predictions range from a square root power law ($D \propto m^{-0.5}$) to an opposite mass dependency of D ($D \propto m^{\beta}$). Experimental studies exhibited consistently a weak power law mass dependency of the diffusion coefficient ($D \propto m^{-\beta}$ with $\beta < 0.5$) for the vast majority of dissolved species and a larger diffusion-induced isotope effect for low weight noble gases ($D \propto m^{-0.5}$). The weak power law mass dependency of D for the species other than low weight noble gases is consistent with the MCTA of diffusion. The MCTA suggests that the weak power law mass dependency of D originates from interplays between strongly mass dependent short-term and mass independent long-term solute-solvent interactions. The larger isotope fractionation for low weight noble gases could be attributed to quantum isotope effects significantly magnifying the aqueous phase diffusion-induced isotope fractionation. Our review shows, that except for low weight noble gases a weak power law mass dependency of D is likely the most adequate assumption for aqueous phase diffusion-induced isotope fractionation in geochemical systems.

* Corresponding author. College of Engineering and Physical Sciences, University of Guelph, 50 Stone Road East, Guelph, Ontario, N1G 2W1, Canada.
E-mail address: pwanner@uoguelph.ca (P. Wanner).

https://doi.org/10.1016/j.chemosphere.2018.12.038
0045-6535/

Contents

1. Introduction

In the past two decades stable isotope methods have emerged as a powerful tool to gain insight into a broad variety of geochemical processes such as rock-water interactions (Frisia et al., 2011; Gimmi et al., 2007; Millot et al., 2010; Voegelin et al., 2012; Waber et al., 2012), partitioning processes (liquid/gas and liquid/solid) (Bouchard et al., 2008; Bouchard et al., 2017; Hunkeler et al., 2011; Jancso and Van Hook, 1974; Jeannottat and Hunkeler, 2012, 2013; Turowski et al., 2003; Wanner et al., 2017) and reactive processes involving both inorganic (Basu et al., 2014; Wanner et al., 2012; Zheng and Hintelmann, 2010) and organic species (Aelion et al., 2010; Badin et al., 2014; Hunkeler et al., 1999, 2008; Palau et al., 2014; Wanner et al., 2016, 2018a, 2018b). The interpretation of spatial and temporal trends of stable isotope ratios requires an understanding of all relevant processes that fractionate isotopes in geochemical systems. Surprisingly, for one of these relevant processes, aqueous phase diffusion, experimental data was only available for a few ions and noble gases until 15 years ago and is still scarce for organic compounds. In the absence of experimental data, the magnitude of isotope fractionation has commonly been estimated based on diffusion models such as Fick's, Maxwell-Stefan's, Einstein's, Langevin's diffusion model or the Mode Coupling Theory Analysis (MCTA) of diffusion (Appelo and Postma, 2005; Chernyavsky and Wortmann, 2007; Chong and Hirata, 1998; Clark and Fritz, 1997; McManus et al., 2002). However, despite using different diffusion models, no review of the conceptualization of the mass dependency of the diffusive transport rate in the different diffusion models can be found in literature.

More recently, multiple experimental studies were conducted to determine the magnitude of aqueous phase diffusion-induced isotope fractionation mainly for inorganic (Bourg et al., 2010; Eggenkamp and Coleman, 2009; Jahne et al., 1987; Kunze and Fuoss, 1962; Pikal, 1972; Richter et al., 2006; Rodushkin et al., 2004; Tempest and Emerson, 2013; Tyroller et al., 2014, 2018; van Zuilen et al., 2016) and to a smaller extent for organic compounds (Jin et al., 2014; LaBolle et al., 2008; Passeport et al., 2014; Rolle and Jin, 2017; Schloemer and Krooss, 2004; Wanner and Hunkeler, 2015; Wanner et al., 2017; Zhang and Krooss, 2001). Despite the publication of several experimental studies, a systematic overview and comparison of the results is lacking. Furthermore, the outcomes of the recent experimental studies were not compared with the conceptualization of the mass dependency of the diffusive transport rate in various diffusion models.

This study aims to review the conceptualization of the mass dependency of the diffusive transport rate in the five most common diffusion models (Fick, Maxwell-Stefan, Einstein, Langevin and MCTA of diffusion). Moreover, the results of the recent experimental studies on isotope fractionation due to aqueous phase diffusion are compiled and the consistency between the experimental data and diffusion models is discussed. Based on this comparison, conclusions are drawn on whether the current models are suitable to predict aqueous phase diffusion-induced isotope fractionation in geochemical systems. Finally, the implications of diffusion-induced isotope fractionation for isotope studies to track origin and fate of solutes is discussed.

2. Conceptualization of mass dependency of the diffusive transport rate in five different diffusion models

For simulating diffusive transport of solutes in the aqueous phase, several diffusion models have been developed. The models can be divided in two groups representing two different concepts: The first group of diffusion models assesses the average behavior of many solute molecules in a solution, while the second group investigates the random trajectory of single solute molecules within the solvent. The former includes Fick's, Maxwell Stefan's diffusion model and the MCTA of diffusion model, while the latter comprises Einstein's and Langevin's diffusion model. In the following sections, each of the model will be discussed including the definitions of the diffusion coefficients followed by the evaluation of how the models conceptualize the mass dependency of the diffusive transport rate.

2.1. Fick's diffusion model

Fick's diffusion model (Fick, 1855) is the most commonly applied model for describing the diffusive transport processes in the aqueous phase. The model postulates two laws of diffusion showing how diffusive fluxes are triggered (first law) and how diffusive fluxes affect the temporal concentration evolution in a given system (second law). Fick's first law of diffusion suggests that the diffusive flux of species i is proportional to concentration gradient and the diffusion coefficient:

$$F_{u,i} = -D_i \frac{\partial C_i}{\partial u} \quad (u = x, y, z) \tag{1}$$

where $F_{u,i}$ (mol/m^2/s) is the diffusive flux in direction x,y and z of species i, D_i (m^2/s) is the diffusion coefficient of species i and $\partial C_i/\partial u$

($mol/m^3/m$) is the spatial concentration gradient along the axis x,y, and z of species i.

In his second law of diffusion Fick (1855) showed that the temporal solute concentration evolution of species i in a given system at position r can be related to the diffusive flux (eq. (1)) according to the following relationship:

$$\frac{\partial C_i(r,t)}{\partial t} = D_i\left(\frac{\partial^2 C_i(r,t)}{\partial x^2} + \frac{\partial^2 C_i(r,t)}{\partial y^2} + \frac{\partial^2 C_i(r,t)}{\partial z^2}\right) \quad (2)$$

Fick's diffusion model provides no information about the mass dependency of the diffusive transport process, as it connects the concentration gradient and the diffusive flux with the diffusion coefficient, which has no direct physical meaning. However, to estimate the values of the Fickian diffusion coefficients several theoretical and empirical definitions can be found in literature, which conceptualize the mass dependency of the diffusion coefficient in different ways (Table 1). For the theoretical definitions of Fick's diffusion coefficient, two approaches are distinguished: the hydrodynamic and the kinetic theory. The hydrodynamic theory assumes that a solute molecule of species i moves through a continuum solvent with a specific viscosity and the diffusion coefficient is described by the Stokes-Einstein relation (Einstein, 1906):

$$D_i = \frac{k_B T}{6\pi\eta R_i} \quad (3)$$

where D (m^2/s) is the diffusion coefficient of species i, k_B (J/K) is the Boltzmann's constant, T (K) is the temperature, η (kg/ms) refers to the dynamic viscosity of the solvent and R_i (m) is the radius of species i.

The hydrodynamic definition of the Fickian diffusion coefficient assumes that the solute is totally coupled with the hydrodynamic modes of motion (i.e. no binary collisions between solvent and solutes are considered) and includes a radius but not a mass dependency (eq. (3)). Thus, the hydrodynamic theory predicts no or only a slight fractionation between isotopically distinct species as an additional neutron increases the mass significantly but not necessarily the radius of a diffusing species (Table 1). In contrast to the hydrodynamic theory, the kinetic theory assumes that the solute molecule of species i diffuses in a dense hard-sphere fluid and the diffusion coefficient is commonly described by the Enskog relation (Alder et al., 1974; Tyrrell and Harris, 1984) (Table 1):

Table 1
Conceptualization of mass dependency of diffusive transport rate in the aqueous phase in different diffusion models.

Diffusion model	Definition of diffusion coefficient (m^2/s)	Mass dependency of diffusion coefficient
Fick	Hydrodynamic theorie: $D_i = \frac{k_B T}{6\pi\eta R_i}$	No mass dependency
	Kinetic theorie: $D_i = \frac{3}{8\rho R_{i0}^2}\frac{1}{g_{i0}(R_i+R_0)}\left(\frac{k_B T}{2\pi\mu_i}\right)^{0.5}$	$D_i \propto m^{-0.5}$
	Worch (1993): $D_i = \frac{3.595\cdot 10^{-11} T}{\eta m_i^{0.53}}$	$D_i \propto m^{-0.53}$
	Wilke and Chang (1955): $D_i = \frac{7.4\cdot 10^{-12}(xM)^{1/2} T}{\eta V_i^{0.6}}$	$D_i \propto m^{\beta}$
	Hayduk and Laudie (1974): $D_i = \frac{13.36\cdot 10^{-9}}{\eta^{1.14} V_i^{0.589}}$	$D_i \propto m^{\beta}$
Maxwell Stefan	$D_{12} = \frac{x_1 x_2}{f_1}\left(\left(\frac{dk_B T}{m_1}\right)^{0.5} - \left(\frac{dk_B T}{m_2}\right)^{0.5}\right)$	$D_i \propto m^{-0.5}$
Einstein	$D_i = \frac{\Delta r^2(t)_i}{6t}$	No information about mass dependency
Langevin	$D_i = \frac{1}{d}\int_0^{\infty} v_i(0)\cdot v_i(t)\cdot dt$	No information about mass dependency
Mode-Coupling Theory Analysis	$D_i = \frac{k_B T}{\zeta^0}$	$D_i \propto m^{-\beta}$

D_i: Diffusion coefficient of species i.
k_B: Boltzmann's constant.
T: Temperature.
η: Dynamic viscosity.
R_0: Radius of solvent.
R_i: Radius of dissolved species i.
ρ: Density of solvent.
$g_{i0}(R_i + R_0)$: Radial distribution function.
μ_i: Reduced mass of solute-solvent pair.
m_i: Molecular mass of species i.
x: Empirical association parameter.
M: Molecular weight of solvent.
V_i: Molar volume of diffusing species i.
v: Velocity.
d: Dimensionality.
ζ^0: Total friction coefficient.
f_1: driving force for diffusion.

$$D_i = \frac{3}{8\rho R_0^2}\frac{1}{g_{i0}(R_i+R_0)}\left(\frac{k_B T}{2\pi\mu_i}\right)^{0.5} \quad (4)$$

where ρ is the density of the fluid, R_0 and R_i is the radius of solvent and the dissolved species i, respectively, $g_{i0}(R_i + R_0)$ is the value of the solute radial distribution function at the point of contact of solute and solvent molecules, and μ_i is the reduced mass of the solute-solvent pair ($\mu_i = m_i M_i/(m_i + M_i)$), where m_i and M_i correspond to the molecular mass of the solute and solvent, respectively.

The kinetic theory (eq. (4)) assumes that the solute motion is decoupled from the hydrodynamic motion of the solvent and describes the diffusive transport processes in terms of binary collision dynamics between solvent and solute molecules similar to the gas phase. Therefore, the kinetic theory predicts an inverse proportionality of the diffusion coefficient to the square root of the reduced mass (μ_i) of the diffusing species i:

$$D_i \propto \mu_i^{-0.5} \quad (5)$$

In the framework of the kinetic theory it can be assumed that the hydrogen-bonded water network acts as "effective particle" with an infinitively large mass ($M_i \gg m_i$) (Bourg and Sposito, 2008; Brennwald et al., 2005; Lippmann et al., 2003; Wanner and Hunkeler, 2015). Thus, the reduced mass can be replaced by the molecular mass of the diffusing species $u_i \rightarrow m_i$ as $m_i + M_i \rightarrow M_i$ (Table 1):

$$D_i \propto m_i^{0.5} \quad (6)$$

where m_i is the molecular mass of the diffusing species i.

In addition to the theoretical definitions of the Fickian diffusion coefficient (hydrodynamic and kinetic), several empirical definitions can be found in literature (Table 1). Worch (1993) suggested the following empirical relationship:

$$D_i = \frac{3.595\cdot 10^{-11} T}{\eta m_i^{0.53}} \quad (7)$$

This definition of the diffusion coefficient is consistent with the kinetic theory showing a mass dependency of the diffusive transport rate, which is roughly inversely proportional to the square root of the molecular mass of the diffusing species i:

$$D_i \propto m_i^{-0.53} \quad (8)$$

Furthermore, Wilke and Chang (1955) and Hayduk and Laudie (1974) empirically correlated diffusion coefficients for diffusing species in liquid water and in non-associated solvents exhibiting the following relationships:

$$D_i = \frac{7.4\cdot 10^{-12}(xM)^{1/2} T}{\eta V_i^{0.6}} \quad (9)$$

$$D_i = \frac{13.36\cdot 10^{-9}}{\eta^{1.14} V_i^{0.589}} \quad (10)$$

where x is the empirical association parameter of the solvent (2.6 for water and 1 for non-polar fluids), M is the molecular weight of the solvent and V_i corresponds to the molar volume of the diffusing species i.

In contrast to Worch (1993), the empirical diffusion coefficients defined by Wilke and Chang (1955) and Hayduk and Laudie (1974) are not directly dependent on the mass but on the volume of the diffusing species (eqs. (9) and (10)). It has been demonstrated that isotopic substitution can have an influence on the molar volume of the diffusing species, especially for deuterated vs. non-deuterated compounds (Bartell and Roskos, 1966; Lacks, 1995). The effect originates from the longer C—H than the C-D bond length due to the greater zero-point energy and the higher vibrational amplitude of the stretching vibrations for C—H compared to C-D bonds. Bartell and Roskos (1966) showed experimentally, that deuterated benzene, toluene, cyclohexane, and methyl cyclohexane have an about 0.3% smaller volume compared to their hydrogenated equivalents. Thus, the empirical diffusion coefficients defined by Wilke and Chang (1955) and Hayduk and Laudie (1974) indirectly lead to a mass dependency of the diffusion coefficient via a power law molar volume dependency:

$$D_i \propto V_i^{-0.6} \quad (11)$$

$$D_i \propto V_i^{-0.589} \quad (12)$$

However, as the isotopically light species have a larger molecular volume than isotopically heavy species, the diffusive transport rate defined by Wilke and Chang (1955) and Hayduk and Laudie (1974) is expected to be faster for heavy compared to light isotopes causing an inverse isotope effect (Table 1). To evaluate if the dependency of the Wilke and Chang (1955) and Hayduk and Laudie (1974) diffusion coefficients on the molecular mass also follows a power law form, as the dependency on the molecular volume (eqs. (11) and (12)), the relationship between the molecular volume and mass needs to be evaluated. The relation can be assessed for deuterated compounds and their hydrogenated equivalents as for these compounds the molecular masses and volumes are well constrained (Bartell and Roskos, 1966) using the following relationship:

$$\frac{V_D}{V} = \left(\frac{m}{m_D}\right)^{\beta} \quad (13)$$

where V_D is the molecular volume of the deuterated compound, V is the volume of its undeuterated equivalent, m_D refers to the molecular volume of the deuterated compound and m is the molecular volume of the compound in its undeuterated state.

The exponent beta in equation (13) shows consistent values for various deuterated/non-deuterated compounds ranging between 0.023 and 0.041 revealing that the molecular volume and mass have a power law relationship. Therefore, the empirical diffusion coefficients defined by Wilke and Chang (1955) and Hayduk and Laudie (1974) have not only a power law dependency on the molecular volume but also on the molecular mass predicting a faster diffusive transport rate for heavy compared to light isotopes of species i:

$$D_i \propto m_i^{\beta} \quad (14)$$

$$D_i \propto m_i^{\beta} \quad (15)$$

The prediction of a faster diffusive transport rate for heavy compared to light isotopes is in contradiction with the kinetic (eq. (4)) and Worch (1993) empirical definition of the diffusion coefficient (eq. (7)), which show a mass dependency of the diffusive transport rate in the opposite way (faster for isotopically light compared to heavy species). Furthermore, the empirical diffusion coefficients defined by Wilke and Chang (1955) and Hayduk and Laudie (1974) are also not consistent with the hydrodynamic theory (eq. (3)) predicting no mass dependency of the diffusive transport rate.

2.2. Maxwell-Stefan's diffusion model

The Maxwell-Stefan diffusion model (Maxwell, 1866; Stefan, 1871) was developed based on the kinetic thermodynamic theory of ideal gases but it has been also applied for liquid solutions (Krishna and Wesselingh, 1997; Liu et al., 2013; Rehfeldt and Stichlmair, 2007, 2010). As opposed to Fick's diffusion model, Maxwell-Stefan's diffusion model provides the advantage that it can be used for describing diffusive transport in multicomponent systems. However, as all other discussed diffusion models only consider a binary solution, the conceptualization of the mass dependency of the diffusive transport rate in the Maxwell-Stefan diffusion model will also be evaluated for a binary solution containing species 1 and 2. The Maxwell-Stefan diffusion model assumes that the driving force for diffusive motion f_1 is the chemical potential gradient of species 1 ($\nabla\mu_1$), which is counterbalanced with the molecular friction between species 1 and 2 (Fig. 1):

$$f_1 = \frac{x_1}{RT}\cdot\nabla\mu_1 = -\frac{x_1 x_2}{D_{12}}(v_1 - v_2) \tag{16}$$

with

$$\mu_1 = \mu_1^0 + RTlnx_1 \tag{17}$$

and

$$v_1 - v_2 = \left(\frac{dk_BT}{m_1}\right)^{0.5} - \left(\frac{dk_BT}{m_2}\right)^{0.5} \tag{18}$$

where $\nabla\mu_1$ is the chemical potential gradient of species 1, R (8.3145 J/molK) is the gas constant, T (K) is the temperature, D_{12} (m^2/s) is the Maxwell-Stephan diffusion coefficient, x_1 and x_2 refer to the mole fractions of species 1 and 2, respectively, $v_1 - v_2$ (m/s) is the velocity difference between species 1 and 2, μ_1^0 is the chemical potential of the pure species 1, μ_1 is the chemical potential for species 1 in a fluid mixture, k_B (J/K) is the Boltzmann's constant and m_1 and m_2 is the molecular mass of species 1 and 2, respectively.

Rearranging equation (16) leads to the definition of the Maxwell-Stefan diffusion coefficient:

$$D_{12} = -\frac{x_1 x_2}{f_1}(v_1 - v_2) = \frac{x_1 x_2}{f_1}\left(\left(\frac{dk_BT}{m_1}\right)^{0.5} - \left(\frac{dk_BT}{m_2}\right)^{0.5}\right) \tag{19}$$

Equation (19) shows that the Maxwell-Stefan diffusion coefficient is proportional to the velocity difference of species 1 and 2 and hence, inversely proportional to the difference of the square root of the molecular mass of species 1 and 2:

$$D_{12} \propto \left(\frac{k_BT}{m_1}\right)^{0.5} - \left(\frac{k_BT}{m_2}\right)^{0.5} \propto m_1^{-0.5} - m_2^{-0.5} \tag{20}$$

When assessing the mass dependency of the diffusive transport rate of species 1 dissolved in the aqueous phase, the mass of species 2 (aqueous phase) can be assumed to be constant and equation (20) can be simplified to:

$$D_{12} \propto \left(\frac{k_BT}{m_1}\right)^{0.5} \propto m_1^{-0.5} \tag{21}$$

Hence, for a dissolved species in the aqueous phase, the Maxwell-Stefan diffusion coefficient is inversely proportional to the square root of the molecular mass of the diffusing species.

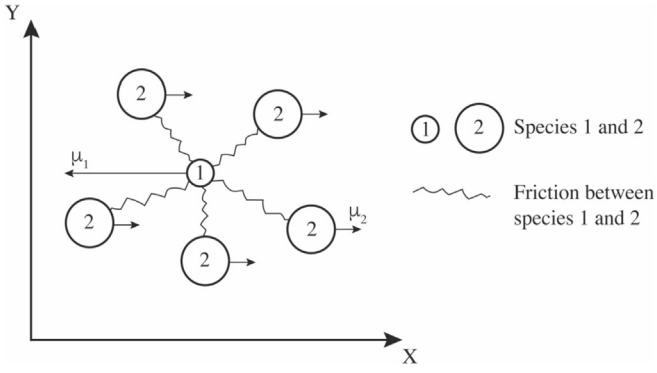

Fig. 1. Schematic illustration of the force balance assumed in the Maxwell-Stefan diffusion model. The force acting per mole of species 1 in x-direction $-d\mu_1/dx$ is equal to the friction between species 1 and 2. Modified after Krishna and Wesselingh (1997).

2.3. Einstein's diffusion model

In contrast to Fick's and Maxwell-Stefan's diffusion model, which are deterministic diffusion models, Einstein's diffusion model (Einstein, 1906) is based on the probabilistic behavior of the solute molecules within a solvent. In particular, Einstein (1906) assessed the probability that a solute molecule of species i changes its position due to its diffusive migration in the solvent. Einstein (1906) considered a time interval δt that is sufficiently long for solute molecules of species i to collide several times with solvent molecules to ensure its random movement, but small enough that it can be considered as infinitesimally small on the macroscopic scale (Fig. 2). Afterwards a probability density function $\varphi(\Delta; \delta t)$ was defined, whereby $\varphi(\Delta; \delta t)d\Delta$ gives the probability that a solute molecule of species i changes its position along the x-axis of a system during δt by an amount between Δ and $\Delta+d\Delta$ due to a collision with a solvent molecule. From the definition of $\varphi(\Delta; \delta t)$, Einstein calculated the average molecular density (concentration) of species i between the spatial interval x and x + dx at time $t+\delta t$ using the following equation:

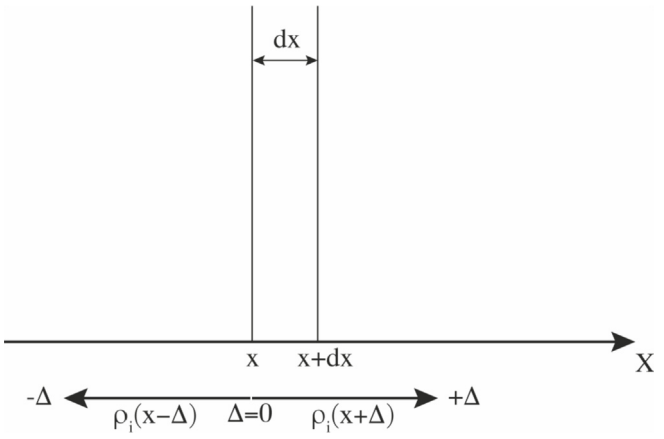

Fig. 2. Schematic illustration of Einstein's perspective on the diffusive transport in the aqueous phase for a one-dimensional case. $\rho_i(x+\Delta)$ and $\rho_i(x-\Delta)$ are the concentrations of species i in positive and negative x direction from the considered dx interval at time t before the collision with the solvent molecules. These concentrations are multiplied with the PDF $\varphi(\Delta; \delta t)$ and then integrated over all Δ values in order to obtain the concentration of species i in the dx interval after the collision with solvent molecules at time $t+\delta t$.

$$\rho_i(x, t+\delta t)dx = \int_{\Delta=-\infty}^{\infty} [\rho_i(x+\Delta, t)dx] \cdot [\varphi(\Delta; \delta t)d\Delta] \quad (22)$$

The first factor in the brackets on the right side of equation (22) indicates the average number of solute molecules of species i at the position x+Δ at time t, which is the average number of solute molecules prior to collision with solvent molecules (Fig. 2). The second term is the probability that the solute molecules will be displaced along the x-axis during the time interval by an amount between Δ and Δ+dΔ and will thus, end up in the x + dx interval at time t+δt. Einstein (1906) integrated equation (22) over all possible Δ values between +∞ and -∞ for obtaining the average number of solute molecules of species i with the x coordinate between x and x + dx at time t+δt. After integrating and rearranging equation (22), Einstein obtained the following equation for describing the diffusive transport process of species i in three dimensions (for details readers are referred to Einstein (1906)):

$$\frac{\partial C_i(r,t)}{\partial t} = D_i\left(\frac{\partial^2 C_i(r,t)}{\partial x^2} + \frac{\partial^2 C_i(r,t)}{\partial y^2} + \frac{\partial^2 C_i(r,t)}{\partial z^2}\right) \quad (23)$$

It is obvious from equation (23) that Einstein (1906) obtained the same equation for describing the diffusive transport process as Fick (1855) (eq. 2). However, although Einstein and Fick derived the same diffusion equation, their perception of aqueous phase diffusion is different. While Fick's diffusion model allows to determine the average number of solute molecules in the interval x,x + dx, at time t, Einstein's diffusion model determines the probability that a particular solute molecule will be in the interval x, x + dx at time t. Einstein (1906) further demonstrated that for a solute molecule of species i initially located at the origin, the solution to equation (23) equals a probability density function corresponding to a Gaussian distribution.

$$f(x,t) = \frac{1}{\sqrt{4\pi D_i t}} e^{-\frac{x^2}{4D_i t}} \quad (24)$$

Moreover, Einstein (1906) showed that the variance of equation (24) is $2D_i t$, equaling the mean square displacement of species i over time:

$$\left\langle \Delta x^2(t) \right\rangle_i = 2D_i t \quad (25)$$

where, $\Delta x(t) = x(t) - x(0)$, whereby the angled brackets indicate an average over all solute molecules of species i. For a three-dimensional case $<\Delta x^2>_i = <\Delta y^2>_i = <\Delta z^2>_i$ and hence, for r = {xyz}:

$$\left\langle \Delta r^2(t) \right\rangle_i = 6D_i t \quad (26)$$

The novelty of Einstein's mean square displacement formula (eq. (26)) was the connection between the macroscopic diffusion coefficient and a measured microscopic quantity, the mean-squared displacement. However, the equation does not state whether and how the diffusion coefficient is related to the mass or volume of the diffusing solute. Einstein deviated such a relation independently from the probabilistic diffusion model based on a deterministic approach (Einstein, 1906). Einstein showed that the diffusion coefficient can be related to the properties of the dissolved species i and the solvent, respectively, (the Boltzmann's constant, the temperature, the dynamic viscosity of the solvent and the radius of the dissolved species i) corresponding to the Stokes-Einstein relation as discussed in section 2.1 (eq. (3)). The Stokes-Einstein relation predicts no or only a small mass dependency of D as an additional neutron increases the mass significantly but not necessarily the radius of the diffusing species i (Table 1).

2.4. Langevin's diffusion model

Similar to Einstein, Langevin's diffusion model focuses on the behavior of single solute molecules within a solvent. The diffusion model was developed by examining a single solute molecule of species i with mass m_i, which is exposed to forces coming from collisions with solvent molecules (Langevin, 1908; Lemons and Gythiel, 1997). In contrast to Einstein's diffusion model, which is based on the probabilistic behavior of a solute molecule, Langevin used Newton's second law to explain the random motion of a solute molecule of species i:

$$m_i \frac{dV(t)}{dt} = -y\nu(t) + X \quad (27)$$

Langevin assumed that the force $F = m_i a$ (Newton's second law; left term eq. (27)), which a solute molecule of species i experiences during collision with solvent molecules, equals the sum of two different forces. The first force (-yv(t); first term right side of eq. (27)) is directly proportional to the velocity of the molecule but in negative direction, whereby the constant y represents the drag force ($y = 6\pi\eta R_i$), which corresponds to the conventional drag force used in hydrodynamics. The second force (X: second term, right side of eq. (27)) corresponds to a randomly fluctuating force, which is independent of the velocity of the moving solute molecule of species i. Langevin used this force cautiously and intuitively because its formal properties were not yet developed and not widely applied at this time, whereas today this force is defined and applied as the Gaussian white noise. For a detailed description of the Gaussian white noise readers are referred to Kuo (1996). In Langevin's diffusion model the definition of the diffusion coefficient of species i is related to the translational velocity of the diffusing species i by using a velocity auto-covariance formula (Gillespie and Seitaridou, 2013) (Table 1):

$$D_i = \frac{1}{d}\int_0^{\infty} \langle \nu(0) \cdot \nu(t) \rangle_i \cdot dt \quad (28)$$

where d is the dimensionality of the system (1D, 2D, 3D), v_i (m/s) is velocity of the diffusing species i and dt corresponds to the infinitesimal time interval.

Equation (28) asserts that the area below the curve $< v(0) \cdot v(t) >_i \cdot dt$ equals the diffusion coefficient of the diffusing species i. Thus, additionally to Einstein (eq. (26)), Langevin obtained a second physical meaning of the diffusion coefficient by relating it to the velocity of the diffusing species i at time 0 and time t, respectively. Langevin's definition of the diffusion coefficient (eq. (28)) does not provide any information about the mass dependency of D. Alternatively the mass dependency of the diffusive transport rate in Langevin's diffusion model can be evaluated by considering the mean square displacement formula. In Langevin's diffusion model the spatial mean square displacement of a solute molecule of species i can be expressed by averaging over the initial velocity of the solute molecule (for details of the deviation of the mean square displacement equations in Langevin's diffusion model readers are referred to Gillespie and Seitaridou (2013)):

$$\left\langle \Delta x^2(t) \right\rangle_i = 2d\frac{k_B T}{y}\left[(t-t_0) - \tau\left(1 - e^{-(t-t_0)/\tau}\right)\right] \quad (29)$$

where k_B (J/K) is the Boltzmann constant, T (K) is the temperature,

$y = 6\pi\eta R_i$ (kg/ms) corresponds to the drag forces, where η is the viscosity of the solvent and R_i (m) is the solute radius of species i, $t - t_0$ (s) is the time interval and τ (s) equals m_i/y where m_i is the molecular mass of species i.

Langevin's mean square displacement formula (eq. (29)) can be decomposed in a long and short-time interval, with respect to the constant τ, which has units of time. When taking a large time interval ($t - t_0 \gg \tau$), the right most term $\tau(1 - e^{-(t-t_0)/\tau})$ in equation (29) becomes zero. Hence, the mean square displacement equation for long-time intervals becomes:

$$\left\langle \Delta r^2(t) \right\rangle_i = 2d\frac{k_B T}{6\pi\eta R_i}(t - t_0) = 2dD(t - t_0) \tag{30}$$

Equation (30) corresponds to Einstein's mean square displacement expression (eq. (26)) showing that during large time intervals ($t - t_0 \gg \tau$) Langevin's and Einstein's mean squared displacement formulas are identical. Hence, for large time intervals ($t - t_0 \gg \tau$) Langevin's diffusion model is not predicting a mass dependency of the diffusive transport rate. To express Langevin's mean square displacement formula for short time intervals ($t - t_0 \ll \tau$) the exponent in equation (29) ($t\text{-}t_0/\tau$) is Taylor-expanded to second order, which results in the following expression (for details reader are referred to Gillespie and Seitaridou (2013)):

$$\left\langle \Delta r^2(t) \right\rangle_i = \frac{dk_B T}{m_i}(t - t_0)^2 \tag{31}$$

Or when taking the square root equation (31) becomes to:

$$\langle \Delta r(t) \rangle_i = \sqrt{\frac{dk_B T}{m_i}}(t - t_0) \tag{32}$$

The term $\sqrt{dk_B T/m_i}$ in equation (32) equals the velocity of a diffusing species i in the gas phase (eq. (18)). Hence, Langevin's model of diffusion assumes that on short time scales the diffusing species i moves ballistically in the aqueous phase as observed in the gas phases and the transport rate is inversely proportional to the square root of the molecular mass of the diffusing species i.

Overall, Langevin's mean square displacement equation (eq. (29)) takes into account both the mass dependent short-term and mass independent long-term solute-solvent interactions. However, for large time intervals ($t - t_0 \gg \tau$), which are used to determine D (eq. (30)), the mean square displacement formula converges to Einstein's formula and Langevin's diffusion model is not predicting a mass dependency of D.

2.5. Mode-coupling theory analysis of diffusion

In addition to the previously described diffusion models (Fick, Maxell-Stefan, Einstein, Langevin), the mode-coupling theory analysis (MCTA) of diffusion is also used to assess the mass dependency of the diffusive transport rate of solutes in the aqueous phase. In the framework of the MCTA of diffusion, the diffusion coefficient of species i is related with the friction coefficient acting on the solute in the aqueous phase (Ali et al., 2002) (Table 1):

$$D_i = \frac{k_B T}{\zeta^0} \tag{33}$$

where D_i (m^2/s) is the diffusion coefficient of species i, k_B (J/K) is Boltzmann's constant, T (K) is the temperature and ζ^0 is the total friction coefficient.

The total friction (ζ^B in eq. (33)) acting on solute molecules of species i in the aqueous phase can be decomposed, by conducting a Laplace transformation (Ali et al., 2001, 2002; Bhattacharyya and Bagchi, 1997):

$$\frac{1}{\zeta^0} = \frac{1}{\zeta^B + \zeta^\rho} + \frac{1}{\zeta^H} \tag{34}$$

where ζ^B and ζ^ρ refer to the friction arising from binary collisions and ζ^H corresponds to the friction due to the coupling of the solute with the hydrodynamic motions of the solvent.

Equation (34) shows that the MCTA of diffusion assumes that the diffusive motion of species i is coupled with the long-term hydrodynamic modes (ζ^H) as well as with the short-term binary collision modes of motions (ζ^B) (Ali et al., 2002; Bhattacharyya and Bagchi, 1997, 2000). According to Bhattacharyya and Bagchi (2000) the diffusive transport rate of the solute is strongly mass dependent during the coupling with the short-term binary collision modes of motion (ζ^B), following the kinetic theory (eq. (4)). On the contrary the coupling of the solute with the long-term hydrodynamic modes of motion (ζ^H) exhibits no mass dependency following the hydrodynamic theory (eq. (3)). Hence, the MCTA of diffusion postulates that the overall mass dependency of the diffusive transport rate is the result of a competition between strongly mass dependent short-term binary-collision modes of motion and weakly mass dependent long-term hydrodynamic modes of motion similar to Langevin's diffusion model. Therefore, the MCTA of diffusion predicts a mass dependency of the diffusion coefficient, which is stronger than in the hydrodynamic theory (eq. (3)) but smaller than in the kinetic theory (eq. (4)) following a more general power law mass dependency with exponent $\beta < 0.5$:

$$\frac{D_H}{D_L} = \left(\frac{m_L}{m_H}\right)^\beta \text{ and hence, } D_i \propto m_i^{-\beta} \tag{35}$$

where D_H and D_L (m^2/s) are the diffusion coefficients of the heavy and light species, respectively, and m_L and m_H are the molecular masses of the heavy and light species, respectively.

2.6. Discussion of different diffusion models

The prediction of the magnitude of aqueous-phase diffusion-induced isotope fractionation in the five discussed diffusion models (Fick, Maxwell-Stefan, Einstein, Langevin, MCTA of diffusion) is not consistent. In the framework of Fick's diffusion model, the different definitions of the diffusion coefficients either neglect a mass dependency of D (hydrodynamic definition of Fickian diffusion coefficient, eq. (3)), show an inverse proportionality to the square root of the molecular mass of the diffusing species (kinetic and empirical definition of the Fickian diffusion coefficient by Worch (1993), eqs. (4) and (7)) or predict a faster diffusive transport rate for heavy compared to light isotopes (empirical definition of Fickian diffusion coefficient by Hayduk and Laudie (1974) and by Wilke and Chang (1955), eqs. (9) and (10)). The Maxwell-Stefan diffusion model predicts an inverse proportionality of D to the square root of the molecular mass of the diffusing species (eq. (16)) similar to the gas phase. This is expected as the theory is based on the kinetic thermodynamic theory of ideal gases. The conceptualization of the mass dependency of D in Maxwell-Stefan's theory of diffusion is consistent with the kinetic (eq. (4)) and the empirical definition of the Fickian diffusion coefficient by Worch (1993) (eq. (7)). In contrast, it is not in agreement with the hydrodynamic (eq. (3)) and the empirical definition of Fick's diffusion coefficient by Wilke and Chang (1955) and Hayduk and Laudie (1974) (eqs. (9) and (10)), which show no or an opposite mass dependency of D i.e. faster for heavy compared to light isotopes. In Einstein's diffusion model, the most significant outcome is the provision of a physical meaning of

D by relating it with the mean square displacement of the diffusing species (eq. (26)). Although this relation is not providing any information about the mass dependency of D, it can be used to evaluate a potential mass dependency of D by measuring the mean square displacement of isotopically distinct species using molecular dynamic (MD) simulations (Bourg and Sposito, 2007; Holmboe and Bourg, 2014) (see details in section "3.2. Discussion of experimental results"). However, this relationship contains some limitations, due to the inverse proportionality to the arbitrarily chosen time interval δt (eq. (26)). When the time interval δt is very small, the solute molecule might not experience enough collisions with the solvent molecules that its movement is random. Thus, during short time intervals, the solute molecule moves nearly straight (ballistic) at a nearly constant speed like in a diluted gas, which is not corresponding to random movement in a liquid phase. Therefore, for small time intervals it is not possible to determine D using Einstein's mean square displacement formula and to assess a potential mass dependency. In addition to Einstein's definition of D, Langevin's diffusion model provides a second physical meaning of D, by showing that D equals the velocity difference of the solute at time t and time zero, respectively (eq. (28)). In contrast to Einstein's diffusion coefficient, this relationship can be used to determine the diffusion coefficient also during short time intervals when the solute moves ballistically but it is not providing any information about the mass dependency of D. However, Langevin's definition of the diffusion coefficient can be used to assess a potential mass dependency of D by measuring the velocities of the diffusing solute at time 0 and time t, respectively for isotopically distinct species using MD simulations similar to Einstein's mean square displacement formula (Bourg and Sposito, 2007, 2008) (see details in section "3.2. Discussion of experimental results"). Moreover, Langevin's diffusion model extends Einstein's mean square displacement formula by considering both short and long-time intervals simultaneously (eq. (29)). This equation suggests an intermediate mass dependency of the diffusive transport between strongly mass dependent short-term and mass independent long-term solute-solvent interactions. However, for large time intervals, during which D is determined, Langevin's mean square displacement formula converges to Einstein's formula and predicts no mass dependency of D being consistent with the hydrodynamic definition of Fickian diffusion coefficient. As opposed to Langevin's diffusion model, the MCTA of diffusion provides an equation for D that includes both the mass dependent short-term solute-solvent interactions and mass independent long-term interactions, respectively (eq. (33)). The MCTA considers different types of friction acting on the solute during both long time and short time intervals, respectively. Hence, for predicting the mass dependency of D, MCTA of diffusion interpolates between the mass independent long-term hydrodynamic friction and the strongly mass dependent short-term friction (eq. (33)). This results in a prediction of an intermediate mass dependency of D following a more general power law mass dependency with $0.0<\beta<0.5$ (eq. (35)). This finding is inconsistent with all other discussed diffusion models (Fick, Maxwell-Stefan, Einstein, Langevin), which predict either no mass dependency, assume an inverse proportionality to the square root of the molar mass of the diffusing species or assert a faster diffusive transport rate for heavy compared to light isotopes.

3. Experimental evaluation of isotope fractionation due to aqueous phase diffusion

In the following sections, experimental studies, which investigated the magnitude of aqueous phase diffusion-induced isotope fractionation are summarized and compared. Furthermore, the outcome of the experimental studies is compared with the prediction of the magnitude of isotope fractionation due to aqueous phase diffusion in the different diffusion models.

3.1. Experimental results

A variety of experimental designs were used to determine the magnitude of isotope fractionation due to aqueous phase diffusion such as polyacrylamide and silica hydrogel gel tubes (Eggenkamp and Coleman, 2009; Jin et al., 2014; Rolle and Jin, 2017; van Zuilen et al., 2016), Graham's type diffusion experiments (Bourg et al., 2010; Richter et al., 2006), refractive index profiling (LaBolle et al., 2008), different types of diffusion cells (Jahne et al., 1987; Kunze and Fuoss, 1962; Oleary, 1984; Pikal, 1972; Rodushkin et al., 2004; Tempest and Emerson, 2013; Tyroller et al., 2014, 2018; Wanner and Hunkeler, 2015) and triaxial flow cells (Schloemer and Krooss, 2004; Zhang and Krooss, 2001). Furthermore, the diffusion experiments covered a large range of temperatures (5°–90° Celsius), pressures (atmospheric to 9 MPa) and solution compositions (distilled water, different types of gels, pore water in sedimentary rock, electrolytic solutions). To quantify the magnitude of isotope fractionation experimentally, beta values (eq. (35)) were derived throughout the different experimental. Kunze and Fuoss (1962), Pikal (1972), Rodushkin et al. (2004), Bourg et al. (2010), Richter et al. (2006), Eggenkamp and Coleman (2009) and van Zuilen et al. (2016) investigated isotope fractionation during aqueous phase diffusion for a wide spectra of dissolved ions (Mg^{2+}, Ca^{2+}, Fe^{2+}, Zn^{2+}, Ba^{2+}, Na^{+}, K^{+}, Li^{+} Cl^{-}, Br^{-}). These studies obtained similar beta values (eq. (35)) ranging between 0.000 and 0.025 (Table 2). Furthermore, Oleary (1984), Jahne et al. (1987) Tyroller et al. (2014), Tyroller et al. (2018) and Tempest and Emerson (2013) determined beta values for neutrally charged gases (CO_2, He, Ar, Ne, Kr, Xe). For Ne, Kr, Xe and carbon isotopes in CO_2 the obtained beta values were similar as for dissolved ions ranging between 0.031 and 0.149 (Table 2). In contrast for Ar the obtained beta values diverged. While Tempest and Emerson (2013) determined a beta value (0.0371) for Ar that is consistent with Ne, Kr, Xe and carbon isotopes in CO_2, Tyroller et al. (2014) obtained a one order of magnitude higher beta value for Ar (0.508; Table 2). In addition to Ar, a one order of order magnitude higher beta value (0.486) compared to Ne, Kr, Xe and carbon isotopes in CO_2 was also observed for He (Jahne et al., 1987).

As opposed to dissolved ions and gases less experimental data are available regarding aqueous phase diffusion-induced isotope fractionation of organic compounds. Some of the experimental studies used deuterated vs. non-deuterated compounds to facilitate the determination of beta values (eq. (35)) for organic compounds. However, the obtained results were not consistent. Some studies obtained beta values close to 0.5 (e.g. 0.455 for ethylbenzene and 0.463 for toluene) (Jin et al., 2014; Rolle and Jin, 2017), detected one order of magnitude lower beta values (e.g. 0.063 for isopropanol and 0.023 for tertiary butyl alcohol) (LaBolle et al., 2008) (Table 2) or observed a diffusion-induced isotope fractionation in the opposite direction (faster diffusive transport rate for deuterated vs. non-deuterated species) obtaining negative beta values (e.g −0.247 for benzene) (Rolle and Jin, 2017). Only a few studies were carried out at natural abundance for organic compounds: Zhang and Krooss (2001) and Schloemer and Krooss (2004) determined the magnitude of carbon isotope fractionation of methane and ethane, whereas Jin et al. (2014) and Wanner and Hunkeler (2015) examined the magnitude of carbon and chlorine isotope fractionation of chlorinated hydrocarbons (1,2-DCA, cDCE and TCE). The obtained beta values were similar to the results obtained for dissolved ions: methane and ethane: 0.036–0.037, 1,2-DCA: 0.023–0.031, cDCE: 0.088, and TCE: 0.024–0.043 (Table 2).

Table 2
Compilation of experimental results for isotope fractionation due to aqueous phase diffusion and most consistent diffusion models.

Species	D_H/D_L	β (eq. (35))	Mass dependency of diffusion coefficient	Most consistent diffusion model	Reference
Na Isotopes	$D_{24Na}/D_{22Na=0.998}$	0.0230	$D \propto m^{-0.0230}$	MCTA	Pikal (1972)
Li Isotopes	$D_{7Li}/D_{6Li=0.9965}$	0.0237	$D \propto m^{-0.0237}$	MCTA	Kunze and Fuoss (1962)
	$D_{7Li}/D_{6Li=0.99772}$	0.015	$D \propto m^{-0.015}$	MCTA	Richter et al. (2006)
Fe Isotopes	$D_{56Fe}/D_{54Fe=0.99991}$	0.0024	$D \propto m^{-0.0024}$	MCTA	Rodushkin et al. (2004)
Zn Isotopes	$D_{66Zn}/D_{64Zn=0.99994}$	0.0019	$D \propto m^{-0.0019}$	MCTA	Rodushkin et al. (2004)
Mg Isotopes	$D_{25Mg}/D_{24Mg=1.00003}$	0.000	$D \propto m^{-0.000}$	Hydrodynamic Fickian diffusion coefficient, MCTA	Richter et al. (2006)
Ba Isotopes	$D_{137Ba}/D_{134Ba=0.99978}$	0.010	$D \propto m^{-0.010}$	MCTA	van Zuilen et al. (2016)
Cl Isotopes	$D_{37Cl}/D_{35Cl=0.99857}$	0.025	$D \propto m^{-0.025}$	MCTA	Richter et al. (2006)
	$D_{37Cl}/D_{35Cl=}0.99841$[a]	0.029	$D \propto m^{-0.029}$	MCTA	Eggenkamp and Coleman (2009)
Br Isotopes	$D_{81Br}/D_{79Br=}0.99920$[a]	0.032	$D \propto m^{-0.032}$	MCTA	Eggenkamp and Coleman (2009)
Ca Isotopes	$D_{44Ca}/D_{40Ca=}0.99957$	0.0045	$D \propto m^{-0.0045}$	MCTA	Bourg et al. (2010)
K Isotopes	$D_{41K}/D_{39K=}0.99790$	0.042	$D \propto m^{-0.042}$	MCTA	Bourg et al. (2010)
He Isotopes	$D_{4He}/D_{3He=}0.870$	0.486	$D \propto m^{-0.486}$	Kinetic Fickian diffusion coefficient, Maxwell-Stefan	Jahne et al. (1987)
Ne Isotopes	$D_{22Ne}/D_{20Ne=}0.99001$	0.104	$D \propto m^{-0.104}$	MCTA	Tyroller et al. (2014)
	$D_{22Ne}/D_{20Ne=}0.9931$	0.0727	$D \propto m^{-0.0727}$	MCTA	Tempest and Emerson (2013)
Ar Isotopes	$D_{40Ar}/D_{36Ar=}0.9479$	0.508	$D \propto m^{-0.508}$	Kinetic Fickian diffusion coefficient, Maxwell-Stefan	Tyroller et al. (2014)
	$D_{40Ar}/D_{36Ar=}0.9961$	0.0371	$D \propto m^{-0.0371}$	MCTA	Tempest and Emerson (2013)
Kr Isotopes	$D_{86Kr}/D_{84Kr=0.9965}$[b]	0.149	$D \propto m^{-0.149}$	MCTA	Tyroller et al. (2018)
Xe Isotopes	$D_{132Xe}/D_{131Xe=0.9997}$[b]	0.039	$D \propto m^{-0.039}$	MCTA	Tyroller et al. (2018)
C Isotopes CO_2	$D_{13CO2}/D_{12CO2=}0.9993$[c]	0.0310	$D \propto m^{-0.0310}$	MCTA	Oleary (1984)
	$D_{13CO2}/D_{12CO2=}0.9991$	0.0387	$D \propto m^{-0.0387}$	MCTA	Jahne et al. (1987)
C Isotopes CH_4	$D_{13CH4}/D_{12CH4=}0.99776$[d]	0.037	$D \propto m^{-0.037}$	MCTA	Zhang and Krooss (2001)
	$D_{13CH4}/D_{12CH4=}0.99783$[e]	0.036	$D \propto m^{-0.036}$	MCTA	Schloemer and Krooss (2004)
C Isotopes C_2H_6	$D_{13C2H6}/D_{12C2H6=}0.99877$[e]	0.038	$D \propto m^{-0.038}$	MCTA	Schloemer and Krooss (2004)
Deuterated and non-deuterated isopropanol (IPA)	$D_{DeutIPA}/D_{IPA} = 0.99305$	0.063	$D \propto m^{-0.063}$	MCTA	LaBolle et al. (2008)
Deuterated and non-deuterated tertiary butyl alcohol (TBA)	$D_{DeutTBA}/D_{TBA} = 0.99741$	0.023	$D \propto m^{-0.023}$	MCTA	LaBolle et al. (2008)
Deuterated and non-deuterated toluene	$D_{DeutTol}/D_{Tol} = 0.96246$	0.455	$D \propto m^{-0.455}$	Kinetic Fickian diffusion coefficient, Maxwell-Stefan	Jin et al. (2014)
Deuterated and non-deuterated ethylbenzene	$D_{Deutethb}/D_{ethb} = 0.96061$	0.455	$D \propto m^{-0.455}$	Kinetic Fickian diffusion coefficient, Maxwell-Stefan	Jin et al. (2014)
Cl Isotopocules[f] cDCE	Not indicated	0.088	$D \propto m^{-0.088}$	MCTA	Jin et al. (2014)
Cl Isotopocules[f] TCE	Not indicated	0.043	$D \propto m^{-0.043}$	MCTA	Jin et al. (2014)
C Isotopocules[f] 1,2-DCA	$D_{1011,2\text{-}DCA}/D_{1001,2\text{-}DCA=}0.99977$	0.023	$D \propto m^{-0.023}$	MCTA	Wanner and Hunkeler (2015)
Cl Isotopocules[f] 1,2-DCA	$D_{1021,2\text{-}DCA}/D_{1001,2\text{-}DCA=}0.99939$	0.031	$D \propto m^{-0.031}$	MCTA	Wanner and Hunkeler (2015)
C Isotopocules[f] TCE	$D_{131TCE}/D_{130TCE=}0.99978$	0.029	$D \propto m^{-0.029}$	MCTA	Wanner and Hunkeler (2015)
Cl Isotopocules[f] TCE	$D_{132TCE}/D_{130TCE=}0.99963$	0.024	$D \propto m^{-0.024}$	MCTA	Wanner and Hunkeler (2015)
Deuterated and non-deuterated benzene	$D_{DeutBen}/D_{Ben} = 1.019$[g]	−0.247	$D \propto m^{0.247}$	Wilke and Chang and Hayduk and Laudie diffusion coefficient	Rolle and Jin (2017)
Deuterated and non-deuterated toluene	$D_{DeutTol}/D_{Tol} = 0.970$[g]	0.463	$D \propto m^{-0.463}$	Kinetic Fickian diffusion coefficient, Maxwell-Stefan	Rolle and Jin (2017)

[a] Average of sevenfold and threefold D_H/D_L measurement for Cl and Br isotopes, respectively reported by Eggenkamp and Coleman (2009).
[b] Average of fourfold D_H/D_L measurements reported by Tyroller et al. (2018).
[c] Average of fivefold D_H/D_L measurements reported by Oleary (1984).
[d] Average of fivefold D_H/D_L measurements reported by Zhang and Krooss (2001).
[e] Average of twofold D_H/D_L measurement reported by Schloemer and Krooss (2004).
[f] The term isotopocules encompasses isotopologues (molecules differing in isotopic composition) as well as isotopomers (molecules having the same number of isotopes but at different positions).
[g] Average of fourfold D_H/D_L measurement reported by Rolle and Jin (2017).

3.2. Discussion of experimental results

With the exception of determined beta values (eq. (35)) for Ar isotopes (0.508) by Tyroller et al. (2014) and for He isotopes (0.486) by Jahne et al. (1987) the conducted experimental studies at natural abundance coherently obtained a weak power law mass dependency of D with beta values ranging between 0.000 and 0.104 (Table 2). This suggests that at natural abundance D shows a weak power law mass dependency for the vast majority of dissolved species. In contrast, the obtained inconsistent beta values for deuterated vs. non-deuterated organic compounds (−0.247 (Rolle and Jin, 2017); 0.455 (Jin et al., 2014); 0.063–0.023 (LaBolle et al.,

2008)) (Table 2) casts some doubt on whether deuterated compounds are representative for studies of isotope fractionation during aqueous phase diffusion at natural abundance. The weak power law mass dependency of D with beta values < 0.5, which was determined by the majority of the experimental studies (Table 2), is not consistent with Fick's, Maxwell-Stefan's, Einstein's and Langevin's diffusion models (Table 1). Therefore, none-of these diffusion models provide a theoretical rationale for the weak power law mass dependency of D observed by the majority of recent experimental studies (Table 2). In contrast, the experimental results were coherent with the MCTA of diffusion. This consistency supports the hypothesis of the MCTA of diffusion that the overall mass dependency of the diffusive transport rate in the aqueous phase results from mass dependent short-term and mass independent long-term interactions between solute and solvent. These solute-solvent interactions can be further investigated using MD simulations.

In the last decade MD simulations have emerged as an additional tool to determine the magnitude of isotope fractionation due to aqueous phase diffusion. The basic concept relies on the quantification of D for isotopically distinct species by using Einstein's mean square displacement formula (eq. (26)) for a time interval being large enough to ensure a random movement of the solute in the solvent or by using Langevin's definition of the diffusion coefficient (eq. (28)). MD simulations with a classical force field were conducted for isotopically distinct ions and noble gases in water by Bourg and Sposito (2007), Bourg and Sposito (2008) and Bourg et al. (2010). The MD results were consistent with the majority of experimental studies (Table 2) and the MCTA of diffusion by showing a weak power law mass dependency of D with beta values ranging between 0.000 and 0.171. Based on the MD simulations, Bourg et al. (2010) revealed that the weak power law mass dependency originates from the interaction between strongly mass dependent short-term binary-collision modes of motion and weakly mass-dependent long-term hydrodynamic modes of motion. On short time scales ($t < 0.05$ ps), the relaxation time of the solvent molecules in the near vicinity of the solute after a solute-solvent collision event is shorter for light compared to heavy solute isotopes. This leads to a higher solute-solvent collision frequency for light compared to heavy solute isotopes and hence, to an acceleration of the diffusive transport for light compared to heavy isotopes causing isotopic separation on short time scales. In contrast, on long time scales ($t > 0.05$ ps) the motion of the solute is coupled with the weakly mass-dependent long-term hydrodynamic modes of motion, whereby the coupling is controlled by the average residence time of water molecules in the first solvation shell of the solute (Bourg et al., 2010; Bourg and Sposito, 2007). A greater residence time of the first solvation shell leads to less frequent binary solute-solvent collisions, and hence, to a stronger coupling of the solute with the weak mass dependent hydrodynamic modes of motion decreasing the mass dependency of D. Despite the consistency of the MD simulations (Bourg et al., 2010; Bourg and Sposito, 2007, 2008) with most of the experimental results, the stronger magnitude of isotope fractionation observed for He isotopes by Jahne et al. (1987) and for Ar isotopes by Tyroller et al. (2014) (Table 2) could not be reproduced. Bourg and Sposito (2008) speculated that for He isotopes quantum isotope effects (quantum tunneling) may have contributed significantly to the magnitude of isotope fractionation causing the larger isotope effect. In contrast for Ar isotopes Bourg and Sposito (2008) considered the influence of quantum tunneling related isotope effects as unlikely as the characteristic length scale of solute/water interactions is more than 25 times the thermal de Broglie wavelength under ambient conditions. Recently, de Magalhaes et al. (2017) conducted *ab initio* molecular simulations (AIMD) to assess the effect of quantum isotope effects on diffusion-induced isotope fractionation in the aqueous phase for noble gases. For He isotopes de Magalhaes et al. (2017) confirmed that quantum isotope effects contribute substantially to the magnitude of isotope fractionation, causing isotope fractionation, that follows the inverse square root relation (eq. (5)) (Table 2) as experimentally observed by Jaehne et al. (1987). Furthermore, de Magalhaes et al. (2017) also detected a considerable impact of quantum isotope effects on Ar isotope fractionation causing a larger isotope effect, which is in agreement with the findings by Tyroller et al. (2014). However, this result it is not consistent with the experimental findings by Tempest and Emerson (2013) (Table 2), which observed a weak mass dependency of D for Ar isotopes, and with the study conducted by Bourg and Sposito (2008). This shows that the magnitude of isotope fractionation for Ar due to aqueous phase diffusion is still under debate.

4. Conclusions

The review of five diffusion models (Fick, Maxwell-Stefan, Einstein, Langevin, MCTA of diffusion) revealed an inconsistency regarding the prediction of the magnitude of diffusion-induced isotope fractionation in the aqueous phase. The conceptualization of the mass dependency of D ranges between the prediction of a mass dependency similar to the gas phase showing a square root power law mass dependency and a prediction of an isotope fractionation in the opposite direction i.e. faster for heavy compared to light isotopes. With the exception for light noble gases (e.g. helium), the vast majority of the experimental studies conducted at natural abundance obtained consistently a weak power law mass dependency of D. As the experiments were conducted at varying temperatures, pressures and in differently composed solutions suggest that the weak power law mass dependency of D is valid for a large range of conditions. The observed weak power law mass dependency of D by the diffusion experiments is consistent with the MCTA of diffusion, which reinforces the validity of the picture of aqueous phase diffusion provided by this model: The magnitude of diffusion induced isotope fractionation is a result of an interplay between strongly mass dependent short-term and mass independent long-term solute-solvent interactions resulting in an overall weak power law mass dependency of D. This model of aqueous phase diffusion-induced isotope fractionation is supported by MD simulation investigations using a classical force field. Furthermore, the observed stronger isotope fractionation for low weight noble gases (e.g. helium) could be explained by the influence of quantum isotope effects (tunneling effects) increasing the magnitude of aqueous phase diffusion-induced isotope fractionation. Overall, our review of diffusion models and experimental studies shows that with the exception for light noble gases a weak power law mass dependency is likely the most appropriate assumption for modelling aqueous phase diffusion-induced isotope fractionation in geochemical systems. Hence, a fairly small aqueous phase diffusion-induced isotope fractionation can be expected causing small interference for source identification and the quantification of reactive processes using stable isotope methods.

Acknowledgments

The authors acknowledge the Swiss National Science Foundation (SNSF) (grant number: 200021E-139877) for their financial support. Furthermore, the authors thank four anonymous reviewers for their constructive comments, which greatly helped to improve the quality of the manuscript.

References

Aelion, C.M., Höhener, P., Hunkeler, D., Aravena, R., 2010. Environmental Isotopes in Biodegradation and Bioremediation. CRC Press, USA.

Alder, B.J., Alley, W.E., Dymond, J.H., 1974. Studies in molecular-dynamics .14. Mass and size dependence of binary diffusion coefficients. J. Chem. Phys. 61, 1415–1420.

Ali, S.M., Samanta, A., Ghosh, S.K., 2001. Mode coupling theory of self and cross diffusivity in a binary fluid mixture: application to Lennard-Jones systems. J. Chem. Phys. 114, 10419–10429.

Ali, S.M., Samanta, A., Ghosh, S.K., 2002. A microscopic theory of tracer diffusivity: crossover to the hydrodynamic limit. Chem. Phys. Lett. 357, 217–222.

Appelo, C.A.J., Postma, D., 2005. Geochemistry, Groundwater and Pollution. CRC Press Amsterdam, Netherlands.

Badin, A., Buttet, G., Maillard, J., Holliger, C., Hunkeler, D., 2014. Multiple dual C-Cl isotope patterns associated with reductive dechlorination of tetrachloroethene. Environ. Sci. Technol. 48, 9179–9186.

Bartell, L., Roskos, R., 1966. Isotope effects on molar volume and surface tension: simple theoretical model and experimental data for hydrocarbons. J. Chem. Phys. 44, 457–463.

Basu, A., Sanford, R.A., Johnson, T.M., Lundstrom, C.C., Löffler, F.E., 2014. Uranium isotopic fractionation factors during U (VI) reduction by bacterial isolates. Geochem. Cosmochim. Acta 136, 100–113.

Bhattacharyya, S., Bagchi, B., 1997. Anomalous diffusion of small particles in dense liquids. J. Chem. Phys. 106, 1757–1763.

Bhattacharyya, S., Bagchi, B., 2000. Power law mass dependence of diffusion: a mode coupling theory analysis. Phys. Rev. 61, 3850–3856.

Bouchard, D., Hunkeler, D., Gaganis, P., Aravena, R., Hohener, P., Broholm, M.M., Kjeldsen, P., 2008. Carbon isotope fractionation during diffusion and biodegradation of petroleum hydrocarbons in the unsaturated zone: field experiment at Vaerlose airbase, Denmark, and modeling. Environ. Sci. Technol. 42, 596–601.

Bouchard, D., Wanner, P., Luo, H., McLoughlin, P.W., Henderson, J.K., Pirkle, R.J., Hunkeler, D., 2017. Optimization of the solvent-based dissolution method to sample volatile organic compound vapors for compound-specific isotope analysis. J. Chromatogr. A 1520, 23–34.

Bourg, I.C., Richter, F.M., Christensen, J.N., Sposito, G., 2010. Isotopic mass dependence of metal cation diffusion coefficient in liquid water. Geochimica et Cosmochimica 74, 2249–2256.

Bourg, I.C., Sposito, G., 2007. Molecular dynamics simulations of kinetic isotope fractionation during the diffusion of ionic species in liquid water. Geochem. Cosmochim. Acta 71, 5583–5589.

Bourg, I.C., Sposito, G., 2008. Isotopic fractionation of noble gases by diffusion in liquid water: molecular dynamics simulations and hydrologic applications. Geochem. Cosmochim. Acta 72, 2237–2247.

Brennwald, M.S., Kipfer, R., Imboden, D.M., 2005. Release of gas bubbles from lake sediment traced by noble gas isotopes in the sediment pore water. Earth Planet. Sci. Lett. 235, 31–44.

Chernyavsky, B.M., Wortmann, U.G., 2007. REMAP: a reaction transport model for isotope ratio calculations in porous media. G-cubed 8.

Chong, S.H., Hirata, F., 1998. Dynamics of solvated ion in polar liquids: an interaction-site-model description. J. Chem. Phys. 108, 7339–7349.

Clark, I.D., Fritz, P., 1997. Environmental Isotopes in Hydrogeology. CRC Press, United States of America.

de Magalhaes, H.P., Brennwald, M.S., Kipfer, R., 2017. Diverging effects of isotopic fractionation upon molecular diffusion of noble gases in water: mechanistic insights through ab initio molecular dynamics simulations. Environ. Sci. Process. Impacts 19, 405–413.

Eggenkamp, H.G.M., Coleman, M.L., 2009. The effect of aqueous diffusion on the fractionation of chlorine and bromine stable isotopes. Geochem. Cosmochim. Acta 73, 3539–3548.

Einstein, A., 1906. Über die von der molekularkinetischen Theorie der Wärme geforderte Bewegung von in ruhenden Flüssigkeiten suspendierten Teilchen Einstein. Ann. Phys. 17, 549–560.

Fick, A., 1855. Über diffusion. Ann. Phys. 170, 59–86.

Frisia, S., Fairchild, I.J., Fohlmeister, J., Miorandi, R., Spötl, C., Borsato, A., 2011. Carbon mass-balance modelling and carbon isotope exchange processes in dynamic caves. Geochem. Cosmochim. Acta 75, 380–400.

Gillespie, D.T., Seitaridou, E., 2013. Simple Brownian Diffuison. Oxford University Press, Oxford.

Gimmi, T., Waber, H., Gautschi, A., Rübel, A., 2007. Stable water isotopes in pore water of Jurassic argillaceous rocks as tracers for solute transport over large spatial and temporal scales. Water Resour. Res. 43.

Hayduk, W., Laudie, H., 1974. Prediction of diffusion-coefficients for non-electrolytes in dilute aqueous-solutions. AIChE J. 20, 611–615.

Holmboe, M., Bourg, I.C., 2014. Molecular dynamics simulations of water and sodium diffusion in smectite interlayer nanopores as a function of pore size and temperature. J. Phys. Chem. C 118, 1001–1013.

Hunkeler, D., Aravena, R., Butler, B.J., 1999. Monitoring microbial dechlorination of tetrachloroethene (PCE) in groundwater using compound-specific stable carbon isotope ratios: microcosm and field studies. Environ. Sci. Technol. 33, 2733–2738.

Hunkeler, D., Aravena, R., Shouakar-Stash, O., Weisbrod, N., Nasser, A., Netzer, L., Ronen, D., 2011. Carbon and chlorine isotope ratios of chlorinated ethenes migrating through a thick unsaturated zone of a sandy aquifer. Environ. Sci. Technol. 45, 8247–8253.

Hunkeler, D., Meckenstock, R.U., Sheerwood Lollar, B., Schmidt, T.C., Wilson, J.T., 2008. A Guide for Assessing Biodegradation and Source Identification of Organic Ground Water Contaminants Using Compound Specific Isotope Analysis. Environmental Protection Agency (EPA), p. 600, 68.

Jahne, B., Heinz, G., Dietrich, W., 1987. Measurement of the diffusion coefficient of sparingly soluble gases in water. J. Geophys. Res. Oceans 92, 10767–10776.

Jancso, G., Van Hook, W.A., 1974. Condensed phase isotope effects. Chem. Rev. 74, 689–750.

Jeannottat, S., Hunkeler, D., 2012. Chlorine and carbon isotopes fractionation during volatilization and diffusive transport of trichloroethene in the unsaturated zone. Environ. Sci. Technol. 46, 3169–3176.

Jeannottat, S., Hunkeler, D., 2013. Can soil gas VOCs be related to groundwater plumes based on their isotope signature? Environ. Sci. Technol. 47, 12115–12122.

Jin, B., Rolle, M., Li, T., Haderlein, S.B., 2014. Diffusive fractionation of BTEX and chlorinated ethenes in aqueous solution: quantification of spatial isotope gradients. Environ. Sci. Technol. 48, 6141–6150.

Krishna, R., Wesselingh, J.A., 1997. The Maxwell-Stefan approach to mass transfer. Chem. Eng. Sci. 52, 861–911.

Kunze, R.W., Fuoss, R.M., 1962. Conductance of alkali halides .3. Isotopic lithium chlorides. J. Phys. Chem. 66, 930–&.

Kuo, H.K., 1996. White Noise Distribution Theory. CRC Press Inc., United States of America, Florida.

LaBolle, E.M., Fogg, G.E., Eweis, J.B., Gravner, J., Leaist, D.G., 2008. Isotopic fractionation by diffusion in groundwater. Water Resour. Res. 44.

Lacks, D.J., 1995. Origins of molar volume isotope effects in hydrocarbon systems. J. Chem. Phys. 103, 5085–5090.

Langevin, P., 1908. Sur la Theorie du Movement Brownien. Comptes Rendus de l'Academie des Sciences, Paris), pp. 530–533.

Lemons, D.S., Gythiel, A., 1997. Paul Langevin's 1908 paper “On the Theory of Brownian Motion”. Ann. Phys. 65, 1079–1081 [Sur la théorie du movement brownien, C.R. Acad. Sci. (Paris) 146, 530–533 (1908)].

Lippmann, J., Stute, M., Torgersen, T., Moser, D., Hall, J., Lin, L., Borcsik, M., Bellamy, R., Onstott, T., 2003. Dating ultra-deep mine waters with noble gases and 36Cl, Witwatersrand Basin, South Africa. Geochem. Cosmochim. Acta 67, 4597–4619.

Liu, X., Schnell, S.K., Simon, J.M., Kruger, P., Bedeaux, D., Kjelstrup, S., Bardow, A., Vlugt, T.J.H., 2013. Diffusion coefficients from molecular dynamics simulations in binary and ternary mixtures. Int. J. Thermophys. 34, 1169–1196.

Maxwell, J.C., 1866. On the dynamical theory of gases. Phil. Trans. Roy. Soc. Lond. 15, 167–171.

McManus, J., Nägler, T.F., Siebert, C., Wheat, C.G., Hammond, D.E., 2002. Oceanic molybdenum isotope fractionation: diagenesis and hydrothermal ridge-flank alteration. G-cubed 3, 1–9.

Millot, R., Scaillet, B., Sanjuan, B., 2010. Lithium isotopes in island arc geothermal systems: Guadeloupe, Martinique (French West Indies) and experimental approach. Geochem. Cosmochim. Acta 74, 1852–1871.

Oleary, M.H., 1984. Measurement of the isotope fractionation associated with diffusion of carbon-dioxide in aqeous-solution. J. Phys. Chem. 88, 823–825.

Palau, J., Cretnik, S., Shouakar-Stash, O., Höche, M., Elsner, M., Hunkeler, D., 2014. C and Cl Isotope Fractionation of 1,2-dichloroethane Displays Unique δ13C/δ37Cl Patterns for Pathway Identification and Reveals Surprising C-cl Bond Involvement during Microbial Oxidation. Environmental Science & Technology.

Passeport, E., Landis, R., Mundle, S.O., Chu, K., Mack, E.E., Lutz, E., Lollar, B.S., 2014. Diffusion sampler for compound specific carbon isotope analysis of dissolved hydrocarbon contaminants. Environ. Sci. Technol. 48, 9582–9590.

Pikal, M.J., 1972. Isotope effect in tracer diffusion - comparison of diffusion coefficients of Na+-24 and Na+-22 in aqueous electrolytes. J. Phys. Chem. 76, 3038–3040.

Rehfeldt, S., Stichlmair, J., 2007. Measurement and calculation of multicomponent diffusion coefficients in liquids. Fluid Phase Equil. 256, 99–104.

Rehfeldt, S., Stichlmair, J., 2010. Measurement and prediction of multicomponent diffusion coefficients in four ternary liquid systems. Fluid Phase Equil. 290, 1–14.

Richter, F.M., Mendybaev, R.A., Christensen, J.N., Hutcheon, I.D., Williams, R.W., Sturchio, N.C., Beloso Jr., A.D., 2006. Kinetic isotopic fractionation during diffusion of ionic species in water. Geochimica et Cosmochimica 70, 277–289.

Rodushkin, I., Stenberg, A., Andrén, H., Malinovsky, D., Baxter, D.C., 2004. Isotopic fractionation during diffusion of transition metal ions in solution. Anal. Chem. 76, 2148–2151.

Rolle, M., Jin, B.A., 2017. Normal and inverse diffusive isotope fractionation of deuterated toluene and benzene in aqueous systems. Environ. Sci. Technol. Lett. 4, 298–304.

Schloemer, S., Krooss, B.M., 2004. Molecular transport of methane, ethane and nitrogen and the influence of diffusion on the chemical and isotopic composition of natural gas accumulations. Geofluids 4, 81–108.

Stefan, J., 1871. Über das Gleichgewicht und die Bewegung insbesondere die Diffusion von Gasgemengen. Sitzungsberichte der Kaiserlichen Akademie der Wissenschaften Wien, 2te Abteilung a 63, 63–124.

Tempest, K.E., Emerson, S., 2013. Kinetic isotopic fractionation of argon and neon during air-water gas transfer. Mar. Chem. 153, 39–47.

Turowski, M., Yamakawa, N., Meller, J., Kimata, K., Ikegami, T., Hosoya, K., Tanaka, N., Thornton, E.R., 2003. Deuterium isotope effects on hydrophobic interactions: the importance of dispersion interactions in the hydrophobic phase. J. Am.

Chem. Soc. 125, 13836–13849.
Tyroller, L., Brennwald, M.S., Busemann, H., Maden, C., Baur, H., Kipfer, R., 2018. Negligible fractionation of Kr and Xe isotopes by molecular diffusion in water. Earth Planet. Sci. Lett. 492, 73–78.
Tyroller, L., Brennwald, M.S., Mächler, L., Livingstone, D.M., Kipfer, R., 2014. Fractionation of Ne and Ar isotopes by molecular diffusion in water. Geochem. Cosmochim. Acta 136, 60–66.
Tyrrell, H., Harris, K., 1984. Diffusion in Liquids: a Theoretical and Experimental Study. Butlerworth, USA.
van Zuilen, K., Müller, T., Nägler, T.F., Dietzel, M., Küsters, T., 2016. Experimental determination of barium isotope fractionation during diffusion and adsorption processes at low temperatures. Geochem. Cosmochim. Acta 186, 226–241.
Voegelin, A.R., Nägler, T.F., Pettke, T., Neubert, N., Steinmann, M., Pourret, O., Villa, I.M., 2012. The impact of igneous bedrock weathering on the Mo isotopic composition of stream waters: natural samples and laboratory experiments. Geochem. Cosmochim. Acta 86, 150–165.
Waber, H., Gimmi, T., Smellie, J., 2012. Reconstruction of palaeoinfiltration during the Holocene using porewater data (Laxemar, Sweden). Geochem. Cosmochim. Acta 94, 109–127.
Wanner, C., Eggenberger, U., Kurz, D., Zink, S., Mäder, U., 2012. A chromate-contaminated site in southern Switzerland—Part 1: site characterization and the use of Cr isotopes to delineate fate and transport. Appl. Geochem. 27, 644–654.
Wanner, P., Hunkeler, D., 2015. Carbon and chlorine isotopologue fractionation of chlorinated hydrocarbons during diffusion in water and low permeability sediments. Geochem. Cosmochim. Acta 157, 198–212.
Wanner, P., Parker, B.L., Chapman, S.W., Aravena, R., Hunkeler, D., 2016. Quantification of degradation of chlorinated hydrocarbons in saturated low permeability sediments using compound-specific isotope analysis. Environ. Sci. Technol. 50, 5622–5630.
Wanner, P., Parker, B.L., Chapman, S.W., Aravena, R., Hunkeler, D., 2017. Does sorption influence isotope ratios of chlorinated hydrocarbons under field conditions? Appl. Geochem. 84, 348–359.
Wanner, P., Parker, B.L., Chapman, S.W., Lima, G.d.P., Gilmore, A., Mack, E.E., Aravena, R., 2018a. Identification of degradation pathways of chlorohydrocarbons in saturated low permeability sediments using compound-specific isotope analysis. Environ. Sci. Technol. 52, 7296–7306.
Wanner, P., Parker, B.L., Hunkeler, D., 2018b. Assessing the effect of chlorinated hydrocarbon degradation in aquitards on plume persistence due to back-diffusion. Sci. Total Environ. 633, 1602–1612.
Wilke, C.R., Chang, P., 1955. Correlation of diffusion coefficients in dilute solutions. AIChE J. 1, 264–270.
Worch, E., 1993. Eine neue gleichung zur berechnung von diffusions koeffizienten gelöster stoffe. Vom Wasser 81, 289–297.
Zhang, T.W., Krooss, B.M., 2001. Experimental investigation on the carbon isotope fractionation of methane during gas migration by diffusion through sedimentary rocks at elevated temperature and pressure. Geochem. Cosmochim. Acta 65, 2723–2742.
Zheng, W., Hintelmann, H., 2010. Isotope fractionation of mercury during its photochemical reduction by low-molecular-weight organic compounds. J. Phys. Chem. 114, 4246–4253.